Synthesis of $Si/Si_{1-x}Ge_x/Si$ heterostructures for device applications using Ge^+ implantation into silicon

A.Nejim, F.Cristiano, R.M.Gwilliam, P.L.F.Hemment
Dept of Electronic & Electrical Engineering, University of Surrey
Guildford, Surrey GU2 5XH, UK
D.A.O.Hope, J. Newey, M.R.Houlton
Defence Research Agency, St Andrews Road
Great Malvern, Worcs. WR14 3PS, UK

Abstract— **The synthesis and doping of $Si/Si_{1-x}Ge_x/Si$ heterostructures by ion implantation is being investigated as an alternative to epitaxial deposition as a means of forming heterostructures for device applications. Test structures with graded $Si/Si_{1-x}Ge_x$ interfaces have been formed in n-type Si wafers by the implantation of 70keV or 140keV Ge^+ ions and doses up to $3\times10^{16}Ge^+$ cm^{-2} to form alloy layers with peak Ge concentrations of up to 11 atomic % . BF_2^+ ions have been implanted to form p-type surface layers and post amorphisation, using 500keV Si^+ into cooled substrates followed by solid phase epitaxial regrowth, has been used to control End of Range (EoR) defects. TEM data from post amorphised samples reveal no extended defects within the alloy region but show a band of EoR defects buried 1μm beneath the surface. The composition, microstructure and junction quality of the alloy layers will be discussed to highlight the potential impact of the process on the manufacturability of advanced bipolar (HBT) devices.**

I. Introduction

The introduction of a deposited epitaxial $Si_{1-x}Ge_x$ base layer in silicon bipolar transistors leads to a valance band offset, enhances the electron transport across the base layer and this, together with high doping levels to reduce the base resistance, has made possible the fabrication of SiGe HBT devices with cut off frequencies higher than 100GHz [1], [2]. Comparable performance to GaAs based transistors has been obtained in the 2-20GHz range [3]. There remain, however, a number of problems regarding the integration and compatibility of SiGe epitaxy with current IC fabrication. High dose germanuim implantation potentially provides an alternative route for the formation of $Si/Si_{1-x}Ge_x/Si$ heterostructures, since ion implantation is a mature, high yield technology which is fully compatible with semiconductor processing. The introduction of germanium into the base/collector junction of silicon bipolar transistors [Si JBT] by ion implantation can be viewed as a single extra step in the fabrication process to produce ion implanted heterojunction bipolar transistor structures (II SiGe HBT)[4].

Device simulations indicate [5] that careful control of the germanium concentration and positioning of the peak of the implanted Ge^+ profile in the vicinity of the base/collector junction should lead to an enhancement of the collector current gain by a factor of up to 10 compared with similar Si BJT. Using a standard self-aligned, double polysilicon process, experimental data from II SiGe HBT [6] devices with 8% Ge peak atomic concentration show a current gain increase by a factor of 1.75 when compared with a silicon reference device.

There remain important issues such as relaxation of the strained layer, enhanced dopant diffusion and the effect of the germanium ion implant induced defects on the electrical characteristics of the base-collector junction. The regrowth of the germanium implanted and amorphised layer leads to a band of dislocation loops (end of range (EoR) defects) below the original crystalline amorphous interface [7], [8], [9]. These defects can act as recombination centres for the minority charge carriers, and their presence in the junction depletion region may lead to a minority carrier leakage current.[10], [11].

II. Aim

In this paper we report an investigation to determine the relaxation threshold and material quality of the $Si_{1-x}Ge_x/Si$ heterostructures formed by Ge^+ implantation into silicon. We have fabricated diodes in these heterostructures to investigate the effect of post amorphisation on p-n junction leakage currents. We also investigate the effect of amorphisation and post amorphisation and regrowth on the boron profiles in these layers.

III. Experimental

In these experiments 3" n-type wafers were implanted with 140keV or 70keV Ge^+ over a range of doses from 1.4×10^{16} to 4×10^{16} as shown in table I. These wafers were then implanted with 40keV BF_2^+ to a dose of $2\times10^{14}/cm^2$ to produce a p-n junction where the peak boron concentration was $5\times10^{19}/cm^3$. Part of these wafers were subsequently post amorphised down to a depth of 1μm using 500keV Si^+ ions which were implanted into wafers cooled to 150K. All wafers were then annealed at 700°C for 20 minutes in a tube furnace under a flow of nitrogen of 1 litre/minute.

Cleaved samples were prepared for Transmission Electron Microscopy (TEM)as described by Faye [12] with fi-

0-7803-3289-X/97$10.00 ©1997 IEEE

nal thinning using a Gatan Ion Beam Miller and were analysed using a JEOL 2000FX at the University of Surrey. Rutherford Backscattering Spectroscopy/Channeling (RBS/C) was performed using 1.5 MeV He^+ ions with an overall system resolution of 14 keV.

The boron distribution in wafers W4, W5 & W6 were determined using a Cameca IMS3F with a 8keV O_2^+ primary beam scanned over an area of 250μm×250μm. The crater depth was measured using a Dectak 3030 with ±10nm uncertainty. Rocking curves from samples W1a, W2 and W3 (table I) were obtained by double crystal X-ray diffractometry (DCXRD) using Cu $K_{\alpha 1}$ radiation. The reflection from the (004) planes was used. The angular rotation between the Bragg angle for the substrate (θ_{Si}) and the Bragg angle for the implanted $Si_{1-x}Ge_x$ layer ($\theta_{Si_{1-x}Ge_x}$) was measured and the perpendicular distortion in the lattice constant ($a_{\perp(Si_{1-x}Ge_x)}$) was calculated [13].

Using two photolithographic steps, mesa diode structures with lateral dimensions ranging from 40μm^2 up to 190μm^2 were fabricated in selected wafers.

IV. Results and analysis

RBS channeling spectra in a < 100 > direction from samples W1a & W1 implanted with $3.8\times10^{16}Ge^+/cm^2$ at 140keV with and without post amorphisation, respectively, are shown in Fig. 1. Good regrowth of the implanted structure is evident in both samples. The minimum yield fraction (χ_{min}) is 3.4% for both samples and the germanium dechanneling fraction (χ'_{Ge}) is 4% for sample W1a and 3.7% for W1.

The only significant difference in the channeled data appears between channels 230 and 240. This peak which is seen only in the data from W1 relates to direct scattering events from a layer at a depth of 220-280nm and is not evident in the post amorphised sample (W1a). The oxygen peak centered on channel 170 is due to a thin layer of SiO_2 on the surface. The germanium profile remains unchanged during post amorphisation and regrowth (Fig.4).

Cross section TEM analysis of these two samples show a band of dislocation loops centered at a depth of 230nm in sample W1 only. (Fig. 3a.) After post amorphisation and regrowth these defects are annihilated in sample W1a and replaced with dislocation loops at a depth of 1μm. No other implantation or strain related defects can be seen in these samples.

For sample W2 implanted with $1.4\times10^{16}Ge^+/cm^2$ at 70keV followed by post amorphisation and regrowth the XTEM does not reveal any defects in the vicinity of the buried $Si_{1-x}Ge_x$ layer. (Fig.3b.) RBS channeling data shown in Fig.2 indicate good long range order and a χ_{min} of 4.1% and χ'_{Ge} of 4.9%. On the other hand sample W3, implanted with a higher dose of $4\times10^{16}Ge/cm^2$ at 70keV followed by post amorphisation and regrowth, shows <111> stacking faults with a high density in the order of $10^{10}/cm^2$. These extend from the surface to a depth of 50nm as can be seen in Fig.3c. RBS channeling data from this sample, shown in Fig.2, indicate higher dechanneling fraction with a χ_{min} of 8.6% and χ'_{Ge} of 11.8%.

DCXRD analysis of samples W1a, W2 & W3 produce a perpendicular lattice constant $a_{\perp(Si_{1-x}Ge_x)}$ of 5.453Åfor W1a, 5.4438Åfor W2 and 5.4659Åfor W3. This indicates that the implanted $Si_{1-x}Ge_x$ layer in all samples show tetragonal distortion with an elastic strain $\epsilon_{\perp(Si_{1-x}Ge_x)}$ of 4052ppm for W1a, 2353ppm for W2 and 6433ppm for W3. It is clear that $\epsilon_{\perp(Si_{1-x}Ge_x)}$ increases with Ge atomic % concentration even though TEM micrographs indicate that W3 is heavily defected and expected to be partially relaxed.

The results from TEM and RBS/channeling analysis confirm that good quality crystalline regrowth has been achieved in the $Si/Si_{1-x}Ge_x$ layers with germanium atomic concentration below 10% for both 140keV and 70keV implanted samples (W1a, & W2). Exceeding this concentration value leads to relaxation of the structure through the formation of a high density of <111> stacking faults nucleated at the peak of the germanium profile, as found in sample W3 which contains a peak germanium concentration of 11%. These results show that the critical dose and, by inference, the volume concentration above which relaxation occurs is within the threshold values of 11 atomic % for 70keV and 9 atomic % for 140keV for the nucleation of stacking faults predicted by Paine etal[14]. Other types of extended defects have been seen in material implanted with higher energy germanium[15].

Selected areas of samples W4 and W4a implanted with 70keV Ge^+ with and without post amorphisation, respectively, and W5, W5a bulk silicon with and without post amorphisation, respectively (table I) were analysed by SIMS to determine the boron profiles. Fig.4 shows a simulated profile of 9keV boron into silicon generated from PDYN (dynamic TRIM) [16] together with experimental data. There is a clear difference between the profiles of boron in W4, which was amorphised only by the Ge^+ implantation prior to the boron implant and W5 where the implantation is into crystalline silicon. At the $1\times10^{16}/cm^3$ concentration level the boron is 100nm deeper in W5 than W4 which we suggest is due to ion channeling. Post amorphisation and regrowth in the silicon only sample (W5a) does not lead to a detectable change in the profile (not shown). However there is extensive broadening of the boron profile in the Ge^+ implanted and post amorphised $Si/Si_{1-x}Ge_x$ sample (W4a) at the $5\times10^{17}/cm^3$ concentration level.

Similarly, samples W6 & W6a (table I) which were implanted with 140keV Ge^+ show shallower distributions in W6 (no post amorphisation) compared to the post amorphised sample which exhibits extensive broading at the $5\times10^{17}/cm^3$ concentration level (not shown). The SIMS profile of germanium although not calibrated for volume concentration remains unchanged after post amorphisation and regrowth in both samples implanted with 140keV Ge^+ (Fig.4) and in samples implanted with 70keV Ge^+ (not shown).

Since the diffusion of an interstitial mediated dopant such as boron [17] is suppressed in strained $Si_{1-x}Ge_x$ material [18], [19] we assume that strain cannot explain the enhanced diffusion seen in the post amorphised $Si_{1-x}Ge_x$

samples. The possibility of inadequate cooling during the Si^+ post amorphisation implant is ruled out since a similar indiffusion in the silicon substrate, which was implanted at the same time, was not seen. Further investigation is needed to clarify this effect.

Current voltage characteristics of mesa diodes with similar dimensions fabricated in samples W7, W7a and reference silicon are shown in fig.5. All the p^+-n junctions show similar forward characteristics but distnictly different leakage currents in reverse bias. The presence of lattice defects within the depletion region gives rise to leakage currents of 4×10^{-3}Amp/cm^{2}and 6.6×10^{-3}Amp/cm^2 at -10V in bulk silicon and $Si/Si_{1-x}Ge_x$ diodes of W7 respectively. In both cases post amorphisation and regrowth reduces the leakage current by almost two orders of magnitude and three orders of magnitude in the bulk silicon and $Si/Si_{1-x}Ge_x$ diodes of W7a respectively, confirming the benefits of post amorphisation. Process optimisation including RTA anneals should improve on these initial data and further reduce leakage currents.

V. Conclusions

Good quality strained $Si/Si_{1-x}Ge_x/Si$ heterostructures with a peak concentration of up to 10 atomic% have been synthesised by high dose Ge^+ ion implantation. Exceeding this limit leads to partial relaxation through the formation of an extensive network of <111> stacking faults nucleated at the peak of the germanium concentration profile. Fabricated diodes in 70keV Ge^+ material show lowest reverse bias leakage currents in the post amorphised material. Boron profiles in post amorphised and regrown 70keV & 140 keV $Si_{1-x}Ge_x$ material show extensive broadening at the $5\times10^{17}/cm^3$ concentration level compared with similar unamorphised $Si_{1-x}Ge_x$ material.

References

[1] E.Kasper, H.Kibbel, H.J.Herzog, and A.Gruhle. *Jpn. J. Appl. Phys.*, 33:2415–2418, 1994.

[2] T.Nakamura and H.Nishizawa. *IEEE Trans Elec Devi*, 42:390–398, 1995.

[3] F.K.LeGoues. *MRS Bulletin*, 21, 1996.

[4] A.Fukami, K.Shoji, T.Nagano, and C.Y.Yang. *Appl. Phys. Lett.*, 57, 1990.

[5] K.Grahn, Z.Xia, P.Kuivalainen, M.Karlsteen, and M.Willander. *Elec. Lett.*, 29(18):1621–1623, 1993.

[6] S.Lombardo, A.Pinto, V.Raineri, P.Ward, and S.U.Campisano. *Elec. Dev. Lett.*, To be published.

[7] K.S. Jones, S. Prussin, and E.R. Weber. *Appl. Phys. A*, 45:1, 1988.

[8] F.Cristiano, A.Nejim, D.Hope, M.Houlton, and P.Hemment. *Nucl. Inst. Meth*, To be published.

[9] A.Nejim, F.Cristiano, P.L.F.Hemment, D.A.O.Hope, J.L.Glasper, C.Pickering, W.Y.Leong, and D.J.Robbins. *Nucl. Inst. Meth*, To be published.

[10] D.Alquier, C.Bergaud, A.Martinez, M.Minondo, C.Jaussaud, L.Laanab, C.Bonafos, and A.Claverie. *IBMM 95*, 1995.

[11] A.Martinez, C.Bergaud, M.Minondo, C.Jassaud, L.Laanab, and A.Claverie. *RTP'94 proceedings*, 1994.

[12] M.M. Faye. PhD thesis, CEMES-LOE/CNRS, 1992.

[13] M.A.G.Halliwell. *Appl. Phys.*, A58:135–140, 1994.

[14] D.C.Paine, D.J.Howard, and N.G.Stoeffel. *J Elec Mater*, 20, 1991.

[15] F. Cristiano, A. Nejim, B.de Mauduit, A. Claverie, and P.L.F.Hemment. To be presented at E-MRS 96 meeting June 1996.

[16] I.R. Chakarov, S.S.Todorov, and D.S.Karpuzov. *Nucl. Inst. Meth*, B69:193–199, 1992.

[17] S.Mizuo and H.Higuchi. *MRS Symp on Impurity Diffusion and Gettering in Semiconductors*, 1984.

[18] N. Moriya, L.C. Feldman, H.S. Luftman, C.A. King, J. Bevk, and B. Freer. *Phys. Rev. Lett.*, 71:883, 1993.

[19] N.E.B.Cowern, P.C.Zalm, P.van der Sluis, D.J.Gravesteijn, and W.B.de Boer. *Phys. Rev. Lett.*, 72, 1994.

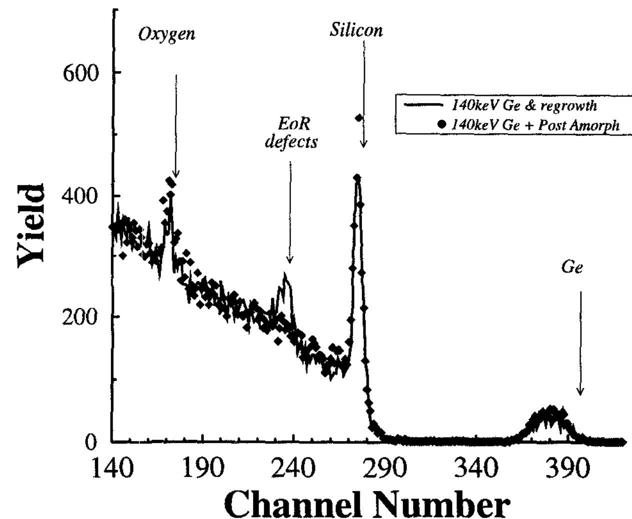

Fig. 1. RBS <100> channeled spectra from two samples implanted with $3.8\times16Ge^+/cm^2$ at 140keV with and without post amorphisation. A band of end of range (EoR) dislocation loops clearly show an increase in the dechanneling fraction between channels 230 and 240

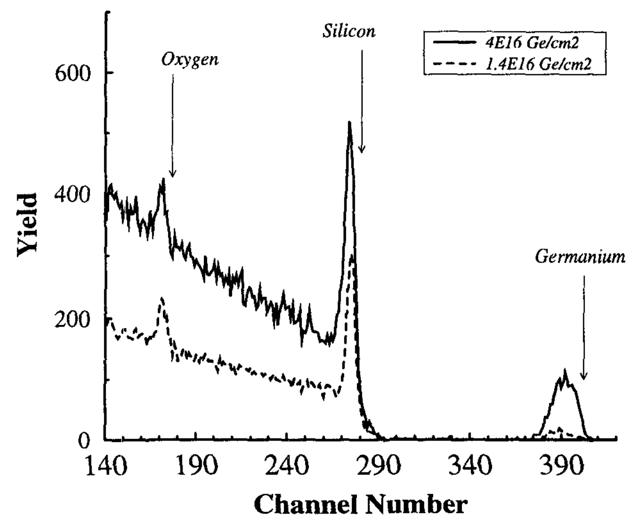

Fig. 2. RBS <100> channeled spectra for two samples implanted with $4E16Ge/cm^2$ and $1.4E16Ge^+/cm^2$ both at 70keV with post amorphisation and regrowth.

TABLE I
TABLE OF SAMPLE DETAILS.

Wafer	Ge^+ Energy keV	Ge^+ Dose $\times 10^{16}cm^{-2}$	BF_2^+ Energy keV	BF_2^+ Dose $\times 10^{14}cm^{-2}$	Post Amorph	Anneal 20min@700°C	Peak atomic % Ge concentration
W1	140	3.8	40	2	No	yes	7
W1a	140	3.8	40	2	Yes	yes	7
W2	70	1.4	-	-	Yes	yes	4
W3	70	4	-	-	Yes	yes	11
W4	70	2.5	40	2	No	yes	10
W4a	70	2.5	40	2	Yes	yes	10
W5	-	-	40	2	No	yes	-
W5a	-	-	40	2	Yes	yes	-
W6	140	3.4	40	2	No	yes	8
W6a	140	3.4	40	2	Yes	yes	8
W7	70	2	40	2	No	yes	8
W7a	70	2	40	2	Yes	yes	8

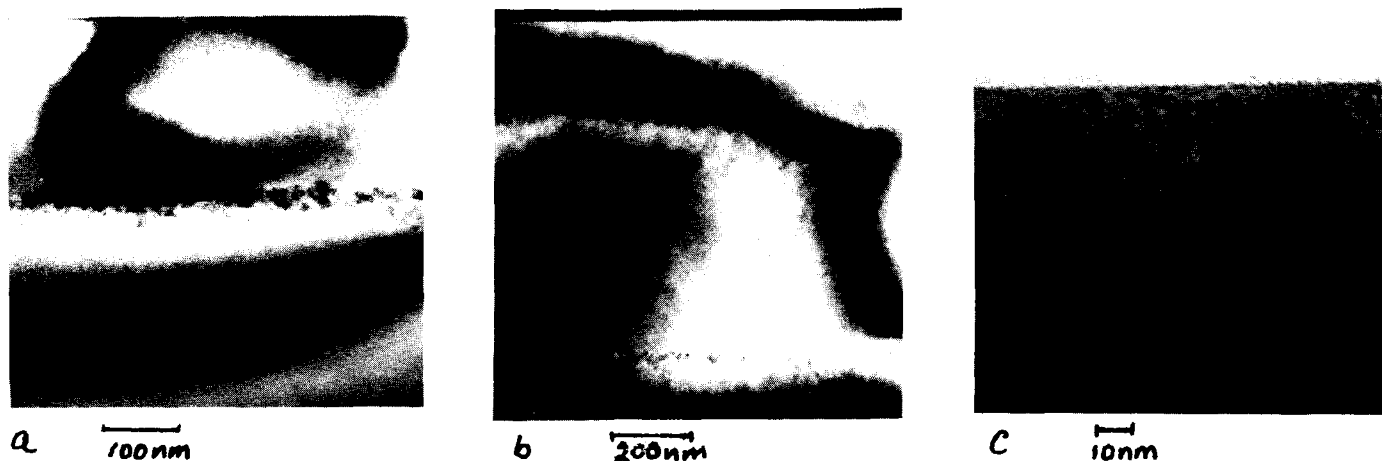

Fig. 3. XTEM micrographs, a) W1(140keV 7% Ge), b) W2 (70keV 4% Ge) & c) W3 (70keV 11% Ge)

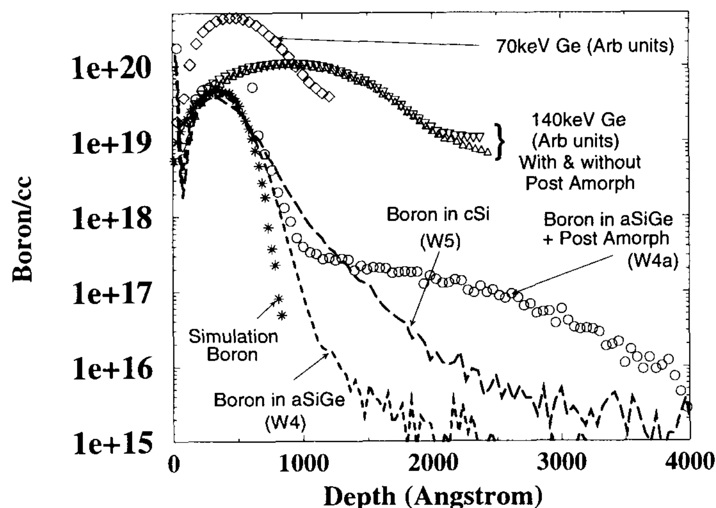

Fig. 4. SIMS data from 70keV & 140keV Ge^+ implanted samples.

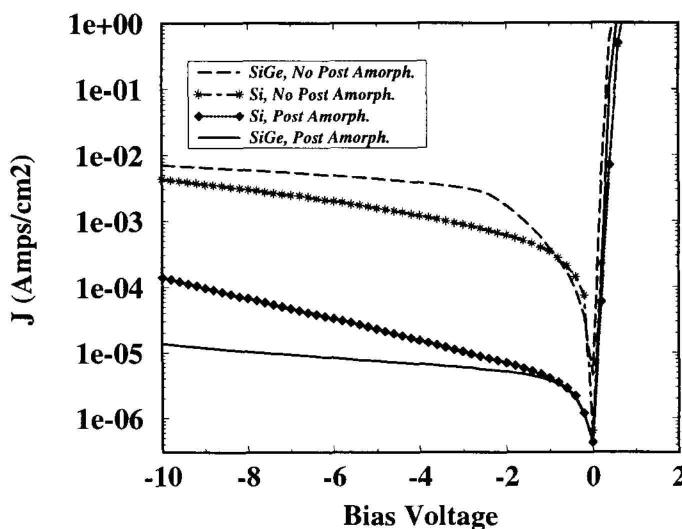

Fig. 5. I-V characteristics of p^+-n junctions fabricated in bulk silicon and W7 & W7a samples implanted with 70keV up to a peak germanium concentration of 8 atomic %